Aerosol Science and Technology

ISSN: 0278-6826 (Print) 1521-7388 (Online) Journal homepage: http://www.tandfonline.com/loi/uast20

Experimental Determination of Supermicrometer Particle Fate Subsequent to a Point Release within a Room under Natural and Forced Mixing

Rachael Jones & Mark Nicas

To cite this article: Rachael Jones & Mark Nicas (2009) Experimental Determination of Supermicrometer Particle Fate Subsequent to a Point Release within a Room under Natural and Forced Mixing, Aerosol Science and Technology, 43:9, 921-938, DOI: 10.1080/02786820903036322

To link to this article: https://doi.org/10.1080/02786820903036322

Published online: 16 Jun 2009.

Aerosol Science and Technology, 43:921–938, 2009

ISSN: 0278-6826 print / 1521-7388 online
DOI: 10.1080/02786820903036322

Experimental Determination of Supermicrometer Particle Fate Subsequent to a Point Release within a Room under Natural and Forced Mixing

Rachael Jones[1] and Mark Nicas[2]
[1]*University of Illinois, School of Public Health, Chicago, Illinois, USA*
[2]*University of California, School of Public Health, Berkeley, California, USA*

The fate of mono-dispersed fluorescein-tagged particles with nominal aerodynamic diameters 3 μm and 14 μm has been measured in a room-scale chamber under natural and forced mixing conditions. The mixing time scales were measured as the time to mixing of carbon monoxide tracer gas. In the forced mixing condition, 3-axis ultrasonic anemometry was used to determine the mean and fluctuating velocity for each vector component at 106 locations. Cumulative deposited fluorescein mass at 61 locations on the chamber floor showed size-dependent and mixing-dependent particle dispersion patterns. More uniform deposition was produced under conditions with relatively shorter mixing time scales, and longer particle settling time scales. A unique data set has been generated for the evaluation of particulate contaminant transport models.

INTRODUCTION

The emergence of SARS coronavirus, pandemic influenza, and multi-drug resistant tuberculosis have stimulated interest in modeling the movement of infectious agents through indoor environments, and the prediction of infection risk. Though viruses and bacteria are typically less than 0.2 μm and 10 μm in diameter, respectively, they are emitted via coughs and sneezes in association with respiratory fluids: These expiratory particles vary in size by several orders of magnitude (Duguid 1946; Loudon and Roberts 1967; Nicas et al. 2005). Modeling the transport of and personal exposures to poly-dispersed particles is challenging due to the treatment of size-specific transport properties, and lack of data for model evaluation.

Recent modeling efforts include the work of Chao and Wan (2006) and Wan et al. (2007), who have modeled the dispersion of cough aerosols with aerodynamic diameters, d_a in the range of 0.3–1000 μm in a ventilated room using computational fluid dynamics (CFD). The influence of ventilation configuration and room layout on exposures of health-care workers to cough aerosols has been explored using CFD simulation (Noakes et al. 2006; Richmond-Bryant 2009). And moving closer to the assessment of infection risk, CFD simulation of SARS coronavirus transmission in a hospital ward has shown a qualitative association between airborne virus concentration (modeled as a tracer gas) and infection incidence (Li et al. 2004). Atkinson and Wein (2008) and Nicas and Jones (in press) have modeled the transmission of influenza within indoor environments by simplifying the spatial distribution of virus in air to focus on the relative significance of exposure via the inhalation of virus aerosol, the direct spray of virus onto the mucus membranes, and contact with virus-contaminated surfaces.

The transport behavior of particles deviates from that of gas-phase contaminants increasingly with particle size: Laboratory-scale experiments have suggested that the deviation is significant for particles with $d_a > 5$ μm (Bémer et al. 2000). There are few full-scale experiments, however, that explore the influence of particle size ($d_a > 5$ μm) on particle transport and fate in indoor environments. Experiments have generally followed three lines of investigation.

The first line has utilized single measurements of contaminants within well-mixed rooms to explore particle loss rates or inter-room contaminant transport. Particle loss rates are key model parameters when rooms are assumed to be well mixed,

Received 29 January 2009; accepted 5 May 2009.
This work was supported by the Center for Advancing Microbial Risk Assessment (CAMRA), funded by the U.S. Environmental Protection Agency Science to Achieve Results (STAR) Program and the U.S. Department of Homeland Security University Programs, grant R83236201. R.M. Jones received additional support from the Center for Disease Control and Prevention Training Program Grant 2T01 CD000189-01. We would like to acknowledge Ms. Seema Bhangar for her assistance with the equipment and experimental advice; Ms. Surakshya Dhakal for her assistance with the fluorescein analysis and tracer gas studies; Dr. Bill Nazaroff for the use of the VOAG and experimental and editorial advice; Dr. Mark Stacey for the use of the fluorometer; and Dr. Mellisa Lunden of Lawrence Berkeley National Laboratory for her time and use of the aerodynamic particle sizer.
Address correspondence to Rachael Jones, School of Public Health, University of Illinois, 2121 W. Taylor Street MC/922, Chicago, IL 60612, USA. E-mail: rjones25@uic.edu

and have been studied in tanks with $d_a < 2$ μm particles (Shimada et al. 1991) and in rooms. Smolík et al. (2005) used outdoor particles with $d_a < 2$ μm to estimate particle loss rates in a bare office. Thatcher et al. (2002) released poly-dispersed particles into, alternatively, a bare, carpeted, and fully furnished room, and measured the concentration evolution of particles with $0.5 < d_a < 10$ μm: The rate of particle loss from air increased with furnishing level and particle size. Multi-room contexts have been used by Lu and Howarth (1996) and Miller and Nazaroff (2001), who measured the evolution of oil smoke particles ($1 < d_a < 5$ μm) and environmental tobacco smoke particles ($d_a < 3$ μm) at one point in each room, respectively.

The second line has explored the assumption of uniformly mixed particle concentration in air. Richmond-Bryant et al. (2006a; 2006b) released particles with $d_a = 3$ μm at two locations in an unfurnished and furnished full-scale test room. Moving the source from near the floor to the ceiling air inlet in an unfurnished room decreased the time until the particles were well-mixed from 600 s to 300 s. In the furnished room, well-mixed conditions were not attained within 600 s.

The third line of investigation has sought to measure the spatial variability in particle concentration. Zhang and Chen (2007) and Murakami et al. (1992) released particles with $d_a < 1$ μm into room-scale chambers and measured particle concentrations in one vertical plane. Sajo et al. (2002) released poly-dispersed cobaltosic oxide ($0.1 < d_p < 15$ μm) in a building lobby, and measured cumulative mass deposition. More closely aligned with the prediction of infection risk was a study by Sze To et al. (2008) in which the investigators measured the concentration of viable bacteriophage released in poly-dispersed particles ($0.3 < d_a < 1000$ μm) as though by a patient in a 3-bed hospital room. These studies are described in more detail.

Sajo et al. (2002) measured the cumulative deposition of cobaltosic oxide at 36 or 56 locations on the floor and on the walls of a building lobby over 90 min subsequent to the bolus point-source release of poly-dispersed cobaltosic oxide. The mechanical ventilation in the room was off, and airspeeds measured by a neutrally buoyant balloon were low, less than 0.25 cm/s. The primary limitation of this study for use in the evaluation of size-resolved particle transport models is the uncertainty about the particle size distribution. Prior to release, the particles were approximately lognormally distributed over the range $0.1 < d_p < 15$ μm, but the release mechanism—a puff of air vertically displaced 10 g of material held in a cup—facilitated particle agglomeration. In addition, the extremely low airspeeds are unlikely to be encountered in mechanically ventilated environments.

Sze To et al. (2008) measured the concentration of viable bacteriophage over 6 min subsequent to a bolus point-source release at 4–5 points at 1.1 m above the floor, and 4–5 points 1.7 m above the floor around three patient beds in a hospital room to characterize patient and health-care worker exposures. The releases mimicked a vertically or horizontally oriented cough emitted by a patient laying in the middle bed: The particle size distribution was similar to that described by Duguid (1946), $0.3 < d_a < 1000$ μm. Bacteriophage concentrations were highly dependent upon the release orientation in the ventilation configuration studied. The assay of viable bacteriophage is a great advance in aerosol research for applications to the study of infection risk, but the utility of this study for model evaluation is limited by the lack of anemometry data and small number of sampling points.

Given the limited research that has characterized the transport and fate of particles with $d_a > 5$ μm, we implemented the following study. In a room-scale chamber, we released fluorescent-tagged mono-dispersed particles with nominal d_a 3 μm and 14 μm under natural and forced mixing conditions. Like Sajo et al. (2002), we used a point-source aerosol release and measured cumulative deposition on the floor. In addition, we measured the time-weighted average fluorescein mass concentration in air, 1.5 m above the floor. Mixing conditions were characterized using carbon monoxide tracer gas, and 3-axis ultrasonic anemometers were used to measure advection and turbulence in the forced mixing condition. Our immediate purpose was to develop a set of data that can be used for the evaluation of contaminant fate and transport models. Given the complexity of transport processes, we elected to use a simple study environment—an unoccupied, unfurnished room-scale chamber. Future work is being planned to experimentally investigate particulate transport in more realistic environments.

METHODS

Experimental Chamber

A room-scale experimental chamber (2.36 m × 2.92 m × 2.39 m high, 16.5 m^3 volume) was constructed using polyethylene sheeting hung over a wood frame in a room inside an office/laboratory building. The chamber floor was the room floor, covered in polyethylene sheeting. The chamber was tightly sealed with duct tape, such that the natural air exchange rate, measured via carbon monoxide concentration decay, was less than 0.01 ACH. The chamber was not thermally insulated. The building mechanical ventilation system was off.

The chamber floor was divided into a grid with length aspect 0.30 m centered at the mid-point of the chamber, such that there were nine rows (denoted 1–9) and seven columns (denoted A–G). The central point of the chamber was in row 5, column D, denoted grid point 5D (Figure 1). The North wall of the chamber (Row 1) was adjacent to an interior building wall. The East wall of the chamber was adjacent to an exterior building wall, and one of the two cardboard-covered windows.

The chamber was equipped with a 0.30 m diameter exhaust fan located in the chamber wall, on the floor at grid point 9D. The fan exhausted chamber air through HEPA filters into the room. The exhaust opening was covered with polyethylene sheeting during the experiments.

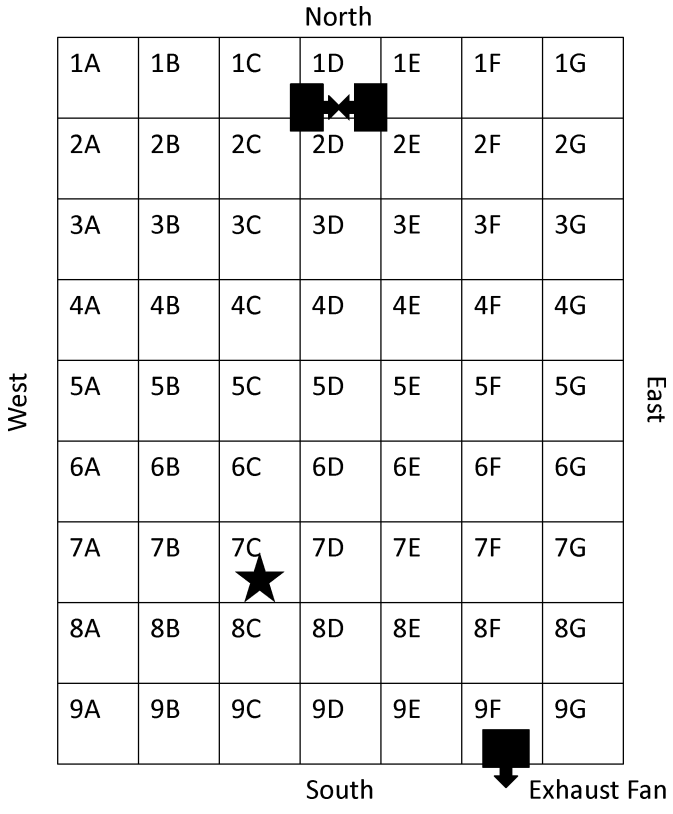

FIG. 1. The floor plan of the experimental chamber. Grid rows are denoted by numbers and columns by letters, with length aspect 0.3 m. Aerosol was released in grid point 7C (star) at height 0.64 m. Forced mixing was induced by two 0.08 m diameter instrument fans on the floor at grid point 1D (boxes, arrows indicate direction of flow). The 0.3 m diameter exhaust fan was located in the wall, on the floor, at grid point 9F (box, arrow indicates direction of flow).

Mixing Conditions

We compared natural and forced mixing conditions. In the natural mixing condition, mixing resulted from thermal convection and the aerosol release mechanism. In the forced mixing condition, two 0.08 m diameter instrument fans were placed on the floor in grid point 1D, such that the centers of the fans were 0.25 m from the North wall. The fans were 0.08 m apart and oriented to blow towards each other. Both fans operated on a 115 V wall outlet. The fan configuration was chosen with the aim of generating forced mixing with relatively homogeneous turbulence and minimal advection in the chamber core.

Mixing Time

A bolus of carbon monoxide was released into the chamber core by emptying a 0.3 L Tedlar bag of 99.5% carbon monoxide into the chamber through a 0.64 cm inner diameter polyvinyl tube. The tube ended at height 1.14 m, above grid point 5D, and was vertically oriented. The release was completed in less than 5 s. Subsequent to the bolus emission at time t = 0, the mixing time, τ_m, was defined as the time t > 0 at which the coefficient of variation (CV) in the carbon monoxide concentration measured at 12 locations on the chamber periphery decreased permanently to less than or equal to 20%. HOBO carbon monoxide monitors (Onset, model H11-011) were hung on the chamber walls at heights 0.46 m or 2.09 m, and recorded the concentration every 5 s. The mixing time, τ_m, was determined for each mixing condition using three replicate trials conducted at different times on three days.

Anemometry

Two three-axis ultrasonic anemometers (R.M. Young, model 81000) measured instantaneous velocity vector components (U, V, W) and the magnitude of the vector, equal to the air speed (U_s), at 4 Hz in the forced mixing condition. Similar measurements were not undertaken in the natural mixing condition because the flows were too low for reliable quantification. The instruments were factory calibrated and had resolution 1 cm/s. Data was logged directly onto two laptop computers. The anemometers were oriented such that the $+u$ velocity was from East to West, $+v$ velocity was from North to South, and $+w$ velocity from floor to ceiling.

The integral time scale of the flow, which measures the duration of velocity dependence, was calculated using a right-hand Riemann sum of the autocorrelation coefficients of instantaneous measurements separated by time lags of 1 s increments, $\tau = [1, 500]$ s. Measurements used to estimate the integral time scale were collected in the chamber core for 60–75 min duration. The integral length scale of the flow, which measures the length aspect of velocity dependence, was calculated using a right-hand Riemann sum of the correlation of instantaneous measurements collected simultaneously on two anemometers separated by distance lag, ξ, in the x-y plane. Measurements used to estimate the integral length scale were collected in the chamber core—centered at 5D aligned in column D (x-axis), and aligned in row 5 (y-axis); and centered at 3D aligned in row 3—for 20 min duration. Measurements were made at 0.1 m intervals,

$$\xi = \{0.36, 0.46, 0.56, 0.66, 0.76, 0.86\}\text{m}.$$

Vertical velocity profiles at four locations did not detect significant vertical patterns in velocity (data not shown): The flow field was characterized in the horizontal plane 0.79 m, 1.14 m, and 1.73 m above the floor for 20 min duration in odd-numbered rows at columns B, D, and F at three different dates and times. Additional measurements were collected for 20 min duration at these heights in rows 1, 5, and 9, at columns A and G to facilitate interpolation of measurements for use in models. Additional measurements were collected for 10 min duration at heights 0.18 m and 0.53 m near the mixing fans, the area of high velocity gradients.

The Reynolds decomposition states that the instantaneous velocities can be decomposed into a mean velocity and a deviation from the mean. Using this approach, the mean velocity components along the orthogonal (x,y,z) axes, ($\overline{u}$, $\overline{v}$, $\overline{w}$), and the

fluctuating velocity components along these axes (σ_u, σ_v, σ_w), were computed as the mean and standard deviation of the time series of instantaneous velocity vector measurements, respectively. The mean air speed ($\overline{U}_s$) and fluctuating air speed (σ_s) were computed as the mean and standard deviation of the time series of instantaneous air speed measurements, respectively.

Aerosol Generation and Release

Fluorescein-tagged neutrally charged particles with nominal d_a of 3 μm and 14 μm were generated using a Vibrating Orifice Aerosol Generator (VOAG, TSI, Model 3450) with Kr-85 charge neutralizer (TSI, Model 3054). The VOAG was operated using a 20 μm orifice, and fluid flow rate of 0.44 mL/min. Two particle fluid solutions were mixed from a fluorescein stock solution of 5 g ammonium fluorescein salt to 1 L of 0.1 M ammonium hydroxide. For the nominal 3 μm particles, the particle fluid solution was 25 mL of fluorescein stock plus 1000 mL of isopropanol. For the nominal 14 μm particles, the particle solution was 300 mL of fluorescein stock, 13 mL oleic acid and 1000 mL of isopropanol. These solutions were expected to produce particles with d_a 3.46 and 14.11 μm when the VOAG was operating at 48 kHz (Berglund and Liu 1973). Exact operating conditions are described in Table 1.

Particle size was checked using an Aerodynamic Particle Sizer (APS). The APS was placed in the chamber for 15–20 min during the release of nominal 3 μm and 14 μm particles. During two consecutive releases of nominal 3 μm particles, the VOAG operated at 44.96 and 44.56 kHz and was expected to produce particles with $d_p = 3.0$ μm, and $d_a = 3.5$ μm at both frequencies. During each release, the APS measured two peaks in particle number concentration in the target particle size range, at d_a 2.46 μm and 3.05 μm. During two consecutive releases of nominal 14 μm particles, the VOAG operated at 48.83 and 48.84 kHz and was expected to produce particles with $d_p = 14.6$ μm and $d_a = 14.0$ μm. During each release, the APS measured the peak particle number concentration in the target size range at $d_a = 14.9$ μm. For both particle sizes, the APS-measured d_a corresponded more closely to the VOAG-expected d_p than to the expected d_a. The difference in particle terminal settling velocity between the APS-measured and VOAG-expected d_a is 26% (0.03 cm/s compared to 0.04 cm/s) and 7% (0.64 cm/s and 0.59 cm/s) for the nominal 3 μm and 14 μm particles, respectively.

TABLE 1
In all experiments (Exp), the Vibrating Orifice Aerosol Generator (VOAG) was operated with a 20 μm orifice, fluid flow rate of 0.44 mL/min, and the specified frequency (Freq). Temperature (Temp) and relative humidity (RH) were measured in the chamber core prior to the aerosol release

		Calculated		Initial	
Exp	Freq (kHz)	d_p (μm)	d_a (μm)	Temp (°C)	RH (%)
		Natural mixing			
T1	49.33	2.95	3.43	19.3	46.5
T2	49.06	2.95	3.43	20.6	42.4
T3	48.91	2.96	3.44	19.3	52.1
T4	48.47	2.97	3.44	19.6	46.3
T5	58.04	13.7	13.3	16.8	52.5
T6	56.67	13.9	13.4	18.8	50.1
T7	56.67	13.9	13.4	18.4	56.2
		Forced mixing			
T8	52.33	2.88	3.34		
T9	50.24	2.93	3.41		
T10	50.78	2.92	3.39		
T11	50.74	2.92	3.39		
T12	54.73	14.0	13.5		
T13	53.84	14.1	13.6	18.1	59.0
T14	52.21	14.2	13.7	16.8	41.5

The VOAG was located outside of the chamber. Aerosol exiting the VOAG passed through the charge neutralizer, and entered the chamber through a 1.83 m long 3.2 cm inner diameter clear polyvinyl tube in carrier air flowing at 50 L/min. The tube was held in the chamber on a ring stand, such that the aerosol was released 0.64 m above the floor in grid point 7C. The tube was angled 25° from vertical, towards the North in column C, and was straight for 0.1 m prior to the release point. In each experiment, aerosol was released into the chamber for 20 min. An experiment was aborted if subsequent to the release, a deflection test indicated that the aerosol was no longer monodispersed. Four successful trials were completed for the nominal 3 μm particles, and three for the nominal 14 μm particles under each mixing condition.

Sample Collection and Analysis

We measured cumulative floor deposition of fluorescein mass using foil-covered cardboard squares that were approximately 0.3 m × 0.3 m. Deposition samplers were placed at 61 grid points on the chamber floor—all points except the points of aerosol release (7C) and the mixing fans (1D).

We measured cumulative wall deposition of fluorescein mass using the deposition samplers in selected experiments under the natural mixing condition. One deposition sampler was attached to each chamber wall, centered at height 1.12 m above the floor in the center of a wall, lengthwise. Thus, the samplers were located above grid points 1D, 5G, 9D, and 5A.

We measured time-weighted-average fluorescein mass concentration at 12 locations 1.5 m above the floor, at approximately standing breathing zone height: The monitoring locations were in even-numbered rows at columns B, D, and F. Samples were collected on downward-facing mixed cellulose ester filters (Millipore, 0.8 μm pore) with support pads held in 25 mm open-face cartridges (SKC, Model 225-1107). Air was drawn through the filters at 2 L/min by personal air sampling pumps (SKC,

AirChek5000 and Universal). The air sampling pumps were located outside of the chamber, and connected to the filters by 0.64 cm inner-diameter polyvinyl tubing. The flow rate of the pumps was measured before and after sample collection (Bios International, Defender 510 M). A flow variation of CV $\leq$5% was accepted. The mean of the two flow rates was used to calculate the sampled air volume.

Sample collection occurred over 90 min: 20 min of aerosol release followed by 70 min of deposition. Sampling was ended by turning off the air sampling pumps, opening the chamber and

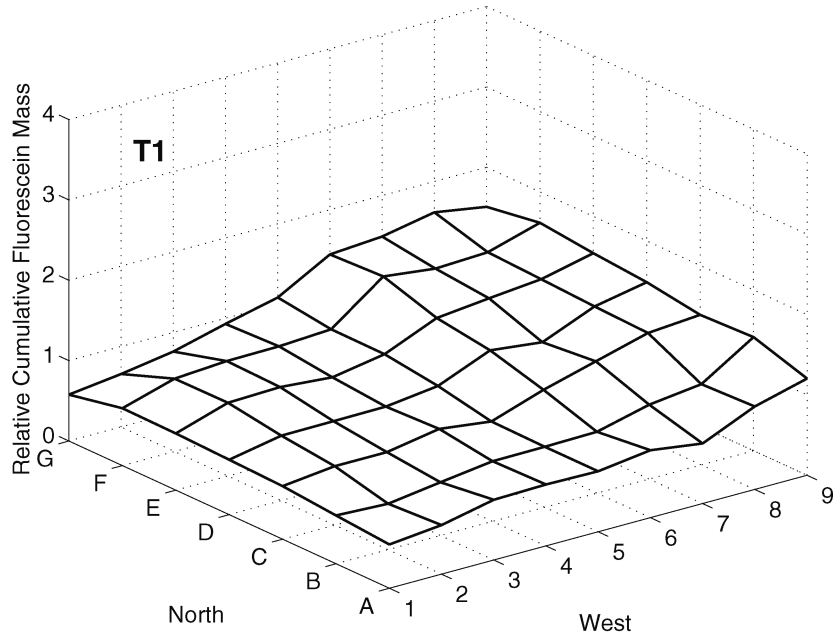

(a)

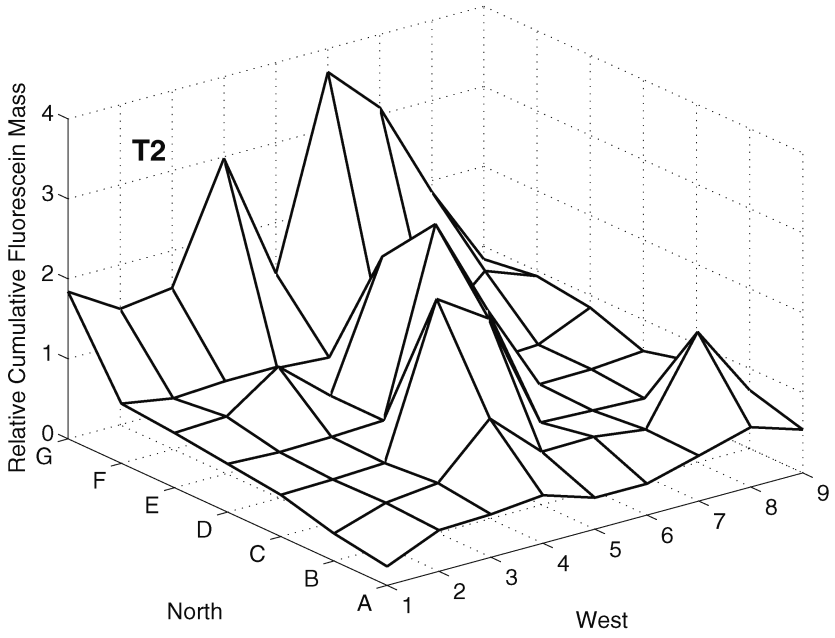

(b)

FIG. 2. Cumulative fluorescein mass deposition, relative to the mean value in each trial, on the chamber floor for particles with nominal $d_a = 3$ μm under natural mixing conditions over 90 min (20 min aerosol release followed by 70 min of deposition). Aerosol was released 0.64 m above the floor at grid point 7C. *(Continued)*

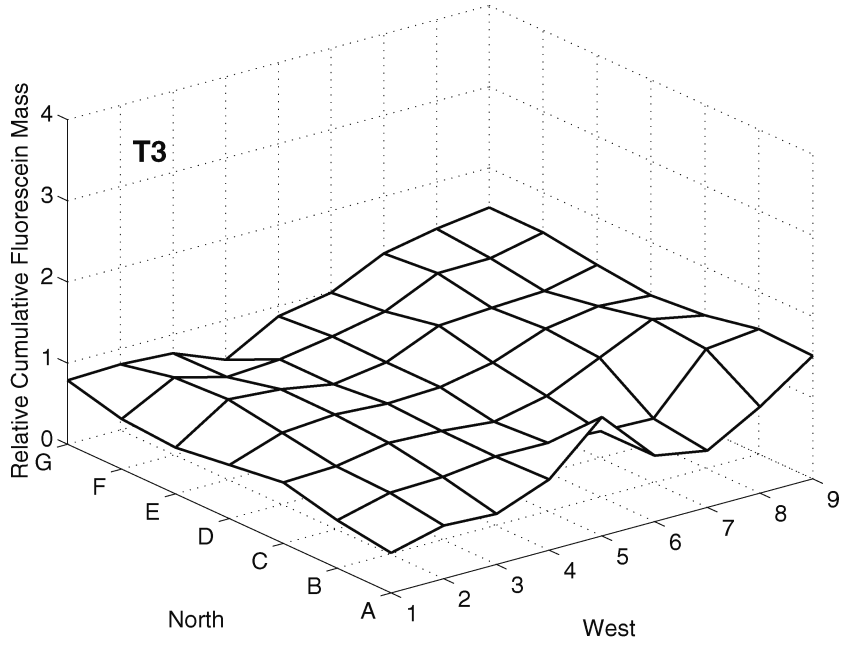

(c)

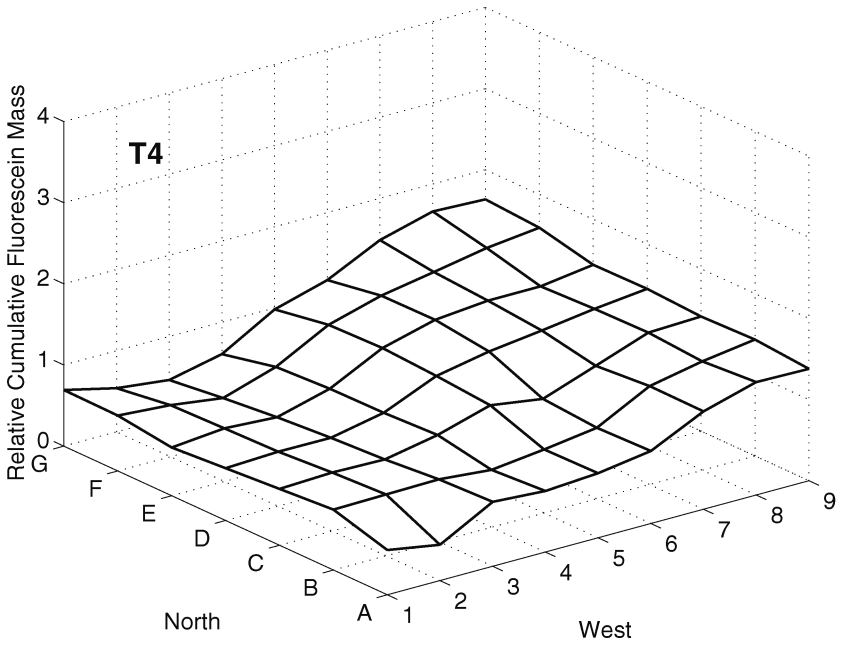

(d)

FIG. 2. (Continued)

removing the deposition samplers on the floor before removing the air samplers. All deposition samplers were removed in less than 3 min.

Sample preparation, storage, and analysis occurred in a windowless room remote from the experiment, but in the same building. Samples were stored in dark cabinets and analyzed within three days of collection. Samples were prepared for analysis by extraction in sodium phosphate buffer (13.4 g sodium phosphate dibasic heptahydride to 1 L deionized water). The central 0.15 m $\times$ 0.15 m area (0.02 m^3) of foil was removed from each deposition sampler for analysis using a razor, tweezers and a cutting template. The 0.02 m^3 foil, or a filter and pad

pair, was placed in a Pyrex dish with 100 mL buffer. Four deposition sampler blanks and one filter and pad pair blank were analyzed per experiment. All samples were gently agitated with the buffer for at least 30 s.

The fluorescein concentration in the buffer of each extracted sample was measured repeatedly using a fluorometer (Turner Designs, Model 10-AU), with gentle agitation for at least 5 s between measurements, until the CV between the two most recent measurements was less than 2.5%. Typically, only two measurements were required. The fluorometer was calibrated to read the fluorescein concentration directly in units of ng/mL. Instrument response over the sample range was linear, with precision of CV $<$ 1%. The concentration of a fluorescein standard in sodium phosphate buffer, and the buffer used for sample extraction were measured after every third sample. Fluorescein concentrations were adjusted for decay in instrument response using a linear regression over the normalized standard measurements within each operating period. The fluorescein mass on the sample was equated with the product of the mean of the two measurements (adjusted) and the volume of buffer (100 mL).

The extraction efficiency for deposition samplers spiked with fluorescein in isopropanol had a mean value of 91% and standard deviation 12% (CV = 13%). The extraction efficiency for filter samples had a mean value of 49% and standard deviation of 28% (CV = 57%). The poor extraction efficiency for the filter samples is likely due to the use of absorbant pads, not quenching. The pads were used due to evidence of sample breakthrough, but fluorescein may have been lost to adsorption into the pad during the extraction from the filter, or to poor extraction from the pad.

Cumulative fluorescein mass on the floor and walls is reported relative to the mean floor deposition value within each experiment. Air sample results were used to calculate the time-weighted average concentration, C_{TWA}: The C_{TWA} is reported relative to the mean value within each experiment.

Experimental blanks, in which no aerosol was introduced to the chamber, were implemented after the first experiment, and then after every three experiments, using 2–4 air samplers and 10 deposition samplers. Samples were below the limit of detection when the chamber had been exhausted by the fan overnight.

RESULTS

Mixing Time

In the natural mixing condition, carbon monoxide was uniformly mixed in the chamber in 54.5, 33.0, and 32.3 min in three replicate trials: $\overline{\tau}_m$ = 39.9 min, with standard deviation 12.6 min (CV = 32%). In the forced mixing condition, carbon monoxide was uniformly mixed in the chamber in 7.1, 8.4, and 7.9 min in three replicate trials: $\overline{\tau}_m$ = 7.8 min, with standard deviation 0.7 min (CV = 8%).

Anemometry

The integral time scale of the flow was 1–3 s, and was longer than the frequency of velocity measurement (4 Hz). The integral length scale of the flow was less than 0.09 m, and was smaller than the chamber grid spacing (0.30 m).

Fluid flow statistics—mean and fluctuating velocities and speed—for the forced mixing condition are indicated in Table A-1, in which repeated measurements at the same location have been combined. Note that in Table A-1, $\overline{U}_s \neq \sqrt{\overline{u}^2 + \overline{v}^2 + \overline{w}^2}$. This is because $\overline{U}_s$ is the average value of the instantaneous speed measurements. Since the computation of U_s is non-linear, $E[f(\mathbf{X})] \neq f(E[\mathbf{X}])$. Apart from the immediate vicinity of the mixing fans, air speeds were low, generally less than 10 cm/s, with fluctuating speeds of approximately 3 cm/s. Near the chamber floor, away from the mixing fans, fluctuating speeds were higher, 6–16 cm/s, than at other heights, though the mean velocities were not elevated. The general advection pattern included low $-\overline{u}$ velocity from East to West (column G to A) and low $\overline{v}$ velocity from North to South (row 1 to 9) throughout the chamber. A downdraft, $-\overline{w}$, and large $|\overline{u}|$ were present to the East and West of the mixing fans, where air was drawn into the fans. High $\overline{w}$ and $|\overline{v}|$ were measured at grid point 2D near the floor, the fan outlet. The trend in $|\overline{u}|$and $|\overline{v}|$ was to decline with distance from the fans, while $\overline{w}$ increased with row number.

Natural Mixing Condition

In three of four experiments (T1, T3, T4) with nominal 3 μm particles, peak cumulative fluorescein mass deposition occurred in the South-West corner of the chamber, near the location of the room window (Figure 2). The deposited mass declined with row number and with column letter. The variation in the cumulative fluorescein mass deposition across the chamber was 30–35% (Table 2). The deposition of 3 μm particles in T2 was very different, with several local maxima present: This variability was confirmed by CV = 76%.

The three experiments with nominal 14 μm particles (T5, T6, T7) measured peak cumulative fluorescein mass deposition in the North-West area of the chamber (Figure 3). The peaks were aligned in column C with the aerosol release (grid point 7C), and were in the direction towards which the release hose was angled. This suggests that the particles followed a projectile path. The CV in the relative cumulative deposited mass was similar for all trials, 59–61% (Table 2).

Wall deposition of fluorescein was negligible (Table A-2): The relative fluorescein mass deposited on the walls, was at least one order of magnitude lower than the lowest relative mass measured on the chamber floor except in T2. In T2, the mass measured on the West chamber wall was approximately equal to the minimum relative fluorescein mass detected on the chamber floor in that trial.

The relative fluorescein mass C_{TWA} measured in all experiments are included in Table A-3. No consistent patterns were measured across the experiments. This may be due to variability

TABLE 2
Cumulative fluorescein mass, relative to the mean value in each trial, deposited on 0.02 m^3 foil floor samplers centered in each grid point over 90 min (20 min aerosol release followed by 70 min of deposition) under natural and forced mixing. Aerosol was released 0.64 m above the floor at grid point 7C. Forced mixing was induced by two 0.08 m diameter instrument fans on the floor, blowing towards each other in grid point 1D

	Relative cumulative fluorescein mass													
	Natural mixing							Forced mixing						
	$d_a \sim 3\ \mu m$				$d_a \sim 14\ \mu m$			$d_a \sim 3\ \mu m$				$d_a \sim 14\ \mu m$		
Grid point	T1	T2	T3	T4	T5	T6	T7	T8	T9	T10	T11	T12	T13	T14
1A	0.54	0.24	0.49	0.55	1.1	0.98	0.95	1.0	1.0	1.0	1.1	0.91	0.94	0.85
1B	0.60	0.34	0.59	0.74	1.6	1.4	1.5	1.0	1.0	1.0	0.96	0.95	0.96	0.88
1C	0.66	0.52	0.75	0.69	1.7	1.6	1.7	1.0	1.0	1.0	0.92	0.97	1.0	0.88
1D						Fan location								
1E	0.71	0.69	0.57	0.59	1.2	1.4	1.7	0.97	1.0	1.1	1.1	1.1	1.2	1.1
1F	0.71	0.74	0.62	0.68	0.83	0.86	0.99	1.0	0.91	1.1	1.1	1.1	1.1	1.1
1G	0.58	1.8	0.79	0.69	0.38	0.32	0.24	1.0	0.96	1.0	1.1	1.1	1.2	1.1
2A	0.61	0.51	0.65	0.69	1.3	1.6	1.2	1.0	1.0	1.1	0.96	0.93	1.0	0.85
2B	0.57	0.55	0.75	0.44	1.8	1.9	1.6	1.1	1.1	1.0	0.94	0.94	0.99	0.87
2C	0.73	0.54	0.78	0.76	1.9	1.9	2.0	1.0	1.0	1.0	0.95	0.90	0.94	0.82
2D	0.81	0.57	0.88	0.72	1.7	1.8	1.9	1.2	1.1	1.0	1.4	2.2	2.0	2.0
2E	0.91	0.72	0.99	0.67	1.3	1.5	1.6	1.0	1.0	1.0	0.94	1.1	1.0	1.1
2F	0.90	0.64	0.95	0.65	1.2	0.99	1.2	1.0	0.99	1.1	1.1	1.1	1.1	1.1
2G	0.66	1.4	0.81	0.63	0.84	0.40	0.36	1.0	1.0	1.0	1.1	1.2	1.2	1.1
3A	0.75	0.54	0.62	0.54	1.2	1.8	1.3	1.0	0.99	1.0	0.91	0.91	0.93	0.84
3B	0.66	0.62	0.77	0.79	1.8	2.1	2.0	1.0	1.0	1.0	0.93	0.94	0.93	0.83
3C	0.73	0.57	089	0.77	2.0	2.0	2.2	1.0	1.0	0.98	0.96	0.90	0.91	0.84
3D	0.81	0.59	0.93	0.71	1.7	1.8	1.9	1.0	0.93	0.98	1.1	1.0	1.0	0.99
3E	0.93	1.2	0.94	0.67	1.3	1.4	1.3	1.0	1.0	1.0	0.94	1.0	0.98	1.1
3F	0.95	0.67	0.78	0.62	1.1	1.0	1.2	1.1	1.0	1.0	0.97	1.1	1.1	1.1
3G	0.76	1.5	0.77	0.55	0.88	0.36	0.68	1.0	1.0	1.0	1.1	1.1	1.1	1.1
4A	0.76	0.60	0.87	0.46	1.3	1.9	1.4	0.99	1.0	1.0	0.93	0.93	0.95	0.84
4B	0.75	1.3	0.85	0.75	1.9	2.0	2.0	1.0	0.96	0.98	1.1	0.92	0.90	0.82
4C	0.85	2.4	0.86	0.71	2.0	2.0	2.1	0.97	0.95	0.95	1.1	0.84	0.88	0.89
4D	0.82	0.62	0.89	0.83	1.8	1.8	1.7	1.0	0.94	0.96	0.94	—	0.89	0.92
4E	0.88	0.62	0.82	0.80	1.3	1.2	1.1	0.95	1.0	1.0	0.94	1.1	0.97	1.1
4F	0.96	0.66	0.82	0.79	1.0	0.89	1.1	1.0	1.0	1.0	0.95	—	1.0	1.1
4G	0.93	3.0	0.51	0.75	0.80	0.31	0.96	1.1	0.99	1.1	1.1	1.1	1.1	1.0
5A	0.75	0.39	1.5	0.61	1.2	1.2	1.3	1.1	1.0	1.0	0.95	0.91	0.90	0.83
5B	0.75	0.66	0.84	0.80	1.7	1.6	1.8	1.0	0.95	0.95	0.94	0.90	0.92	0.86
5C	0.76	2.0	0.80	0.78	1.8	1.9	1.7	0.97	0.98	0.93	0.93	0.94	0.94	0.87
5D	0.90	2.9	0.92	1.0	1.6	1.6	1.3	1.0	0.95	0.95	0.94	1.0	0.95	0.95
5E	0.99	2.2	0.92	1.1	1.2	0.99	0.79	0.98	0.95	0.98	1.1	1.1	0.97	1.1
5F	0.99	0.62	0.93	1.1	0.89	0.83	0.95	1.0	0.99	1.0	1.1	1.1	1.0	1.2
5G	1.1	1.4	0.87	1.1	0.73	0.28	0.90	0.96	1.1	1.0	1.1	1.1	1.1	1.0
6A	0.84	0.39	0.81	0.98	1.1	0.98	1.3	0.93	0.97	0.89	0.90	0.85	0.90	0.84
6B	0.76	067	0.81	0.89	1.4	0.99	1.3	0.94	0.94	0.91	0.92	0.92	0.89	0.86
6C	0.98	0.55	0.94	0.88	1.6	1.6	1.2	0.92	0.92	0.88	1.1	0.97	0.94	0.90
6D	1.2	1.7	1.0	0.93	1.1	1.2	0.78	0.96	0.95	0.90	0.93	1.0	0.97	0.96

(Continued on next page)

TABLE 2
Cumulative fluorescein mass, relative to the mean value in each trial, deposited on 0.02 m^3 foil floor samplers centered in each grid point over 90 min (20 min aerosol release followed by 70 min of deposition) under natural and forced mixing. Aerosol was released 0.64 m above the floor at grid point 7C. Forced mixing was induced by two 0.08 m diameter instrument fans on the floor, blowing towards each other in grid point 1D *(Continued)*

	Relative cumulative fluorescein mass													
	Natural mixing							Forced mixing						
	$d_a \sim 3\ \mu m$				$d_a \sim 14\ \mu m$			$d_a \sim 3\ \mu m$				$d_a \sim 14\ \mu m$		
Grid point	T1	T2	T3	T4	T5	T6	T7	T8	T9	T10	T11	T12	T13	T14
6E	1.3	0.65	1.2	1.2	0.90	0.82	0.57	0.96	0.99	1.0	0.92	1.1	0.94	1.1
6F	1.5	0.81	1.1	1.3	0.72	0.72	0.74	0.96	1.1	1.0	1.1	1.0	1.0	1.2
6G	1.4	3.7	0.99	1.3	0.64	0.42	0.91	1.0	1.0	1.0	1.0	1.0	1.2	0.97
7A	0.75	0.57	0.70	1.2	1.1	0.47	0.81	0.92	0.83	0.91	0.95	0.78	0.80	0.78
7B	0.92	0.59	0.79	1.2	1.0	0.51	0.41	1.1	0.86	0.87	0.88	0.87	0.86	0.85
7C						Release location								
7D	1.1	0.54	1.3	1.2	0.21	0.73	0.36	0.96	0.98	1.0	0.96	0.98	0.91	1.0
7E	1.3	0.52	1.2	1.3	0.49	0.61	0.42	0.99	1.1	1.0	0.95	1.0	0.99	1.2
7F	1.4	0.58	1.4	1.3	0.52	0.64	0.58	1.0	1.0	1.0	0.91	1.1	1.1	1.2
7G	1.5	3.1	1.3	1.4	0.52	0.51	0.82	0.98	1.0	1.1	1.1	1.0	1.1	1.0
8A	1.0	0.75	1.1	1.5	0.74	0.27	0.39	0.95	0.92	1.1	0.94	0.75	0.77	0.76
8B	1.3	1.6	1.5	1.4	0.53	0.34	0.24	0.97	0.96	0.83	0.98	0.84	0.78	0.82
8C	1.4	0.50	1.5	1.3	0.14	0.38	0.17	0.92	1.0	0.90	1.0	0.91	0.87	0.98
8D	1.4	0.56	1.4	1.4	0.05	0.43	0.18	0.97	1.0	0.94	1.0	1.0	0.91	1.2
8E	1.4	0.56	1.3	1.4	0.09	0.48	0.27	1.0	1.0	1.0	1.0	1.1	0.91	1.2
8F	1.6	1.2	1.4	1.4	0.32	0.50	0.48	1.0	1.0	1.0	0.92	1.1	1.0	1.2
8G	1.2	1.9	1.4	1.5	0.33	0.54	0.70	1.1	1.0	1.1	1.1	0.96	1.2	0.97
9A	1.4	0.54	1.5	1.7	0.59	0.20	0.25	1.0	0.98	1.0	1.0	0.72	0.71	0.72
9B	1.4	0.73	1.5	1.4	0.26	0.23	0.13	0.99	0.99	1.0	0.92	0.83	0.84	0.85
9C	1.4	0.77	1.4	1.4	0.11	0.29	0.16	1.0	1.0	0.97	0.89	0.90	0.92	1.0
9D	1.5	0.61	1.3	1.4	0.06	0.32	0.17	0.96	1.0	1.0	1.1	0.94	0.97	1.1
9E	1.5	0.85	1.4	1.4	0.06	0.38	0.25	1.0	1.0	1.0	0.93	0.99	0.99	1.1
9F	1.6	0.93	1.5	1.4	0.11	0.41	0.40	0.98	1.1	1.1	0.96	1.0	1.1	1.1
9G	1.5	0.84	1.5	1.5	0.23	0.42	0.44	1.0	1.1	1.0	1.0	0.92	1.2	0.90
CV (%)	31	76	30	35	59	61	60	4	5	5	9	19	18	19

in the experimental conditions, or the high variability in the sample extraction efficiency.

Forced Mixing Condition

In the four experiments with nominal 3 μm particle released under the forced mixing condition (T8, T9, T10, T11), relatively uniform cumulative fluorescein mass deposition was measured throughout the chamber (Figure 4). In T11, a peak was present at grid point 2D, immediately in front of the mixing fans. In T8, a peak was also present at this location, but was much smaller in magnitude. The magnitude of the variability across the chamber was small, with CV 4–9% (Table 2).

The three experiments with nominal 14 μm particles released under forced mixing condition (T12, T13, T14) measured similar patterns of fluorescein mass deposition the pattern: A sharp peak in mass deposition was present at grid point 2D, immediately in front of the mixing fans, and deposition was relatively uniform throughout the rest of the chamber (Figure 5). The CV was 18–19% for all experiments (Table 2). For T12, values are missing for grid points 4D and 4F due to inaccurate recording of the sample identification code during analysis.

The relative fluorescein mass C_{TWA} measured in all experiments are included in Table A-3. Experiments with the nominal 14 μm particles measured higher C_{TWA} near the release point (7C). No pattern is apparent for the nominal 3 μm particles.

DISCUSSION

We measured the fate of fluorescein-tagged neutrally charged particles with nominal d_a of 3 μm and 14 μm emitted from a point source within a room-scale chamber under natural and forced mixing. Our primary focus was characterizing the spatial variability in particle fluorescein mass deposition on the chamber floor. We also measured the TWA airborne particle fluorescein mass concentrations at 12 chamber locations, but we judge the air sampling data is not reliable due to the high variability in extraction efficiency.

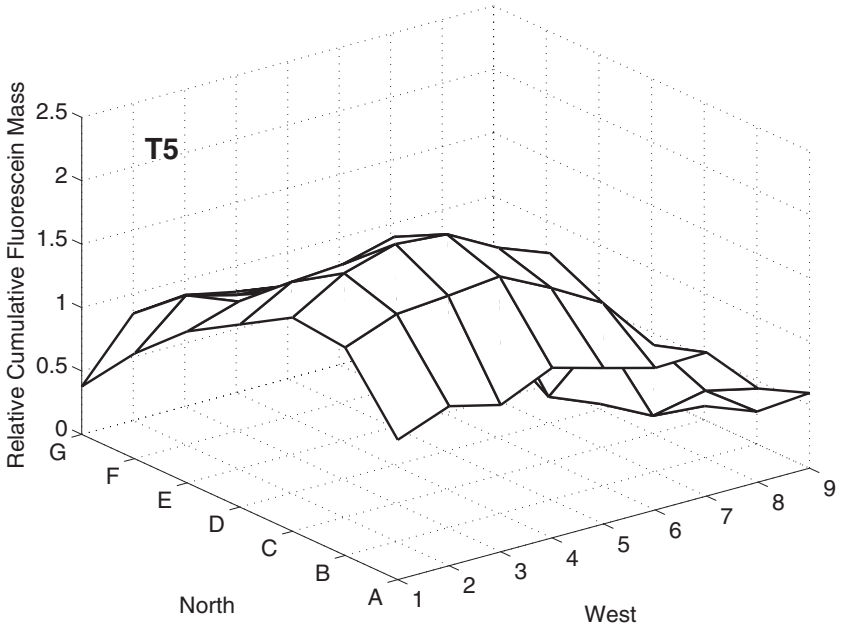

(a)

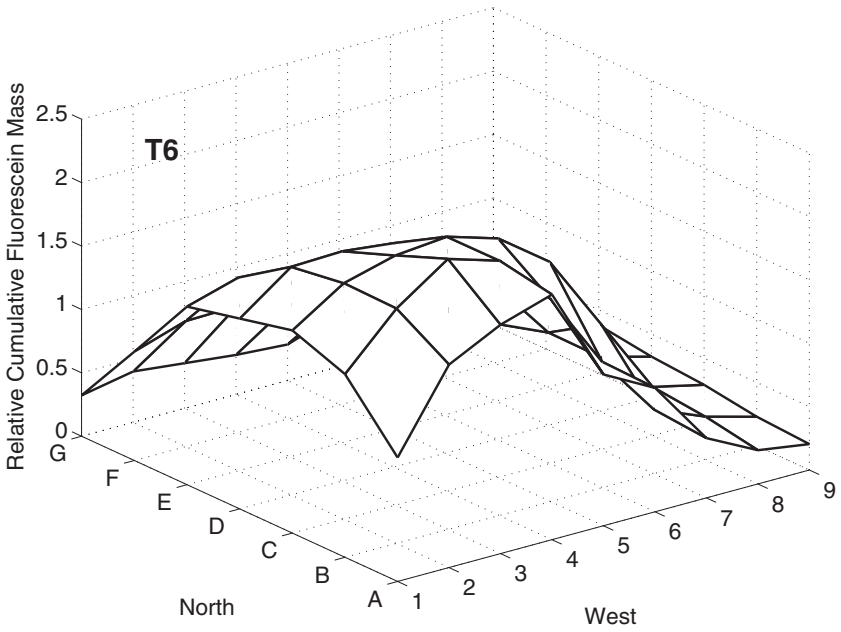

(b)

FIG. 3. Cumulative fluorescein mass deposition, relative to the mean value in each trial, on the chamber floor for particles with nominal $d_a = 14$ μm under natural mixing conditions over 90 min (20 min aerosol release followed by 70 min of deposition). Aerosol was released 0.64 m above the floor at grid point 7C. *(Continued)*

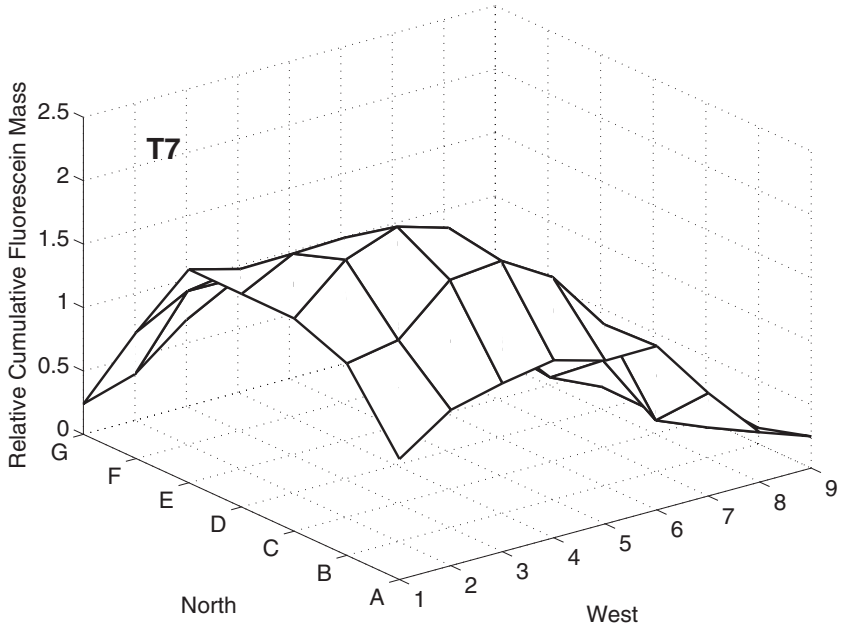

(c)

FIG. 3. (Continued)

In this experimental system, there are four time scales of importance: the time scales of exposure, ventilation, mixing (τ_m), and settling (τ_s). The exposure time scale equates to the duration of the experiments, 90 min. The ventilation time scale is the inverse of the air exchange rate, 100 h (1/0.01 ACH). The ventilation time scale is so much greater than the exposure time scale that the influence of ventilation on the system can be ignored. The mixing time scale for gaseous contaminants equates to the measured mixing time: $\overline{\tau}_m = 39.9$ min under natural mixing, and $\overline{\tau}_m = 7.8$ min under forced mixing. The settling time scale equates to the time required for a particle to be removed from room air due to gravitational acceleration, and is based on the room height, $H = 2.39$ m, and terminal settling velocity, V_{TS}. Particles with $d_a = 3$ μm have $V_{TS} = 0.017$ m/min; and particles with $d_a = 14$ μm have $V_{TS} = 0.36$ m/min. The settling time scale is defined as $\tau_s = H/V_{TS}$. Substitution gives $\tau_s = 141$ min for 3 μm particles and $\tau_s = 6.6$ min for 14 μm particles. The mixing time scale for particles was not measured directly. The mixing time scale of gaseous contaminants, however, describes the turbulent and advective mixing experienced by particles. It is this mixing, balanced by settling, and the exposure duration, that characterize the expected transport of particles in this environment.

Under the natural mixing condition for the 3 μm particles, τ_m (39.9 min) was much shorter than τ_s (141 min). This circumstance signifies that 3 μm particles will be well mixed throughout room air before appreciable settling occurs: Particle deposition is predicted to be somewhat uniform throughout the room. This prediction is consistent with Figure 2, which depicts a fairly uniform deposition of the 3 μm particles in three of four experiments (T1, T3, T4); the CV of the relative deposited masses was 30–35%. Due the lack of thermal regulation in the chamber, convective air currents may have caused the gradient in deposition toward the southwest corner of the chamber. Conversely, under natural mixing condition for the 14 μm particles τ_s (6.6 min) was much shorter than τ_m (39.9 min). This circumstance signifies that 14 μm particles will appreciably settle before they can be dispersed throughout the room air: Particle deposition is predicted to be fairly nonuniform in the room. This prediction is consistent with Figure 4, which depicts nonuniform deposition of the 14 μm particles: Deposition was localized around grid points 2C and 3C, and the CV of the relative deposited masses was 59–61%.

Under the forced mixing condition for the 3 μm particles, τ_m (7.8 min) is much shorter than τ_s (141 min). This circumstance signifies that 3 μm particles will be well mixed throughout room air before appreciable settling occurs: Particle deposition is predicted to be somewhat uniform throughout the room. This prediction is consistent with Figure 3, which depicts fairly uniform deposition of the 3 μm particles; the CV the relative deposited masses was 4–9%. Air speeds were relatively homogeneous, and fluctuating velocities approximately isotropic in the room core (Table A-1), which would be expected to facilitate uniform dispersion in the chamber. The magnitude of the fan-induced air flow would mask convective air currents. For the 14 μm particles, τ_m (7.8 min) is approximately equal to τ_s (6.6 min). This circumstance signifies that particles will be well mixed throughout room air before appreciable settling occurs: Particle

deposition is predicted to be somewhat uniform throughout the room. This prediction is consistent with Figure 5, which depicts fairly uniform deposition of the 14 μm particles, except at grid point 2D, immediately in front of the mixing fans. This peak may be the result of particle momentum causing the particle trajectory to deviate from the streamlines in this area of high velocity gradients.

The exposure time scale, 90 min, was shorter than the settling time scale for the 3 μm particles, and longer than that for the 14 μm particles. Given that the mixing scales for both the natural

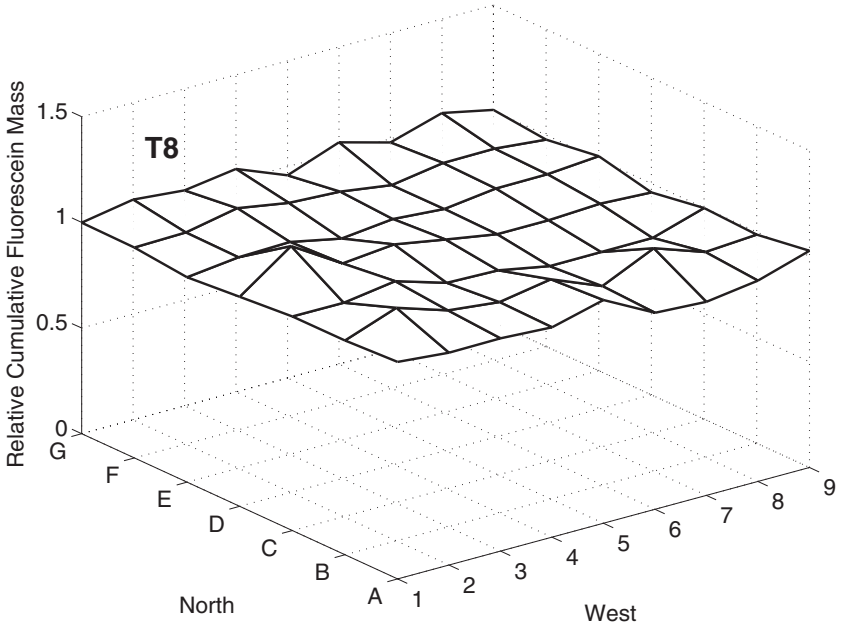

(a)

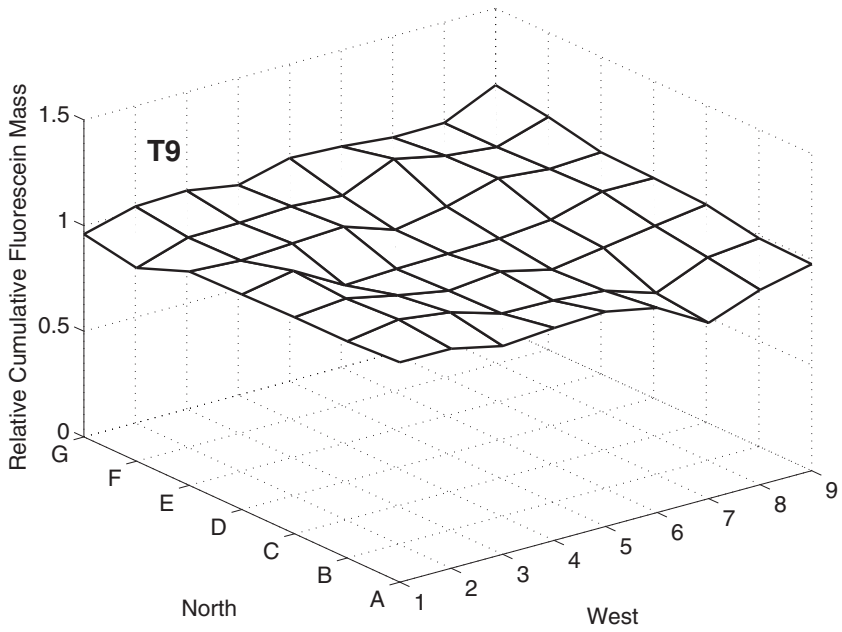

(b)

FIG. 4. Cumulative fluorescein mass deposition, relative to the mean value in each trial, on the chamber floor for particles with nominal $d_a = 3$ μm under forced mixing conditions over 90 min (20 min aerosol release followed by 70 min of deposition). Aerosol was released 0.64 m above the floor at grid point 7C. Mixing was induced by two fans blowing towards each other on the floor in grid point 1D. *(Continued)*

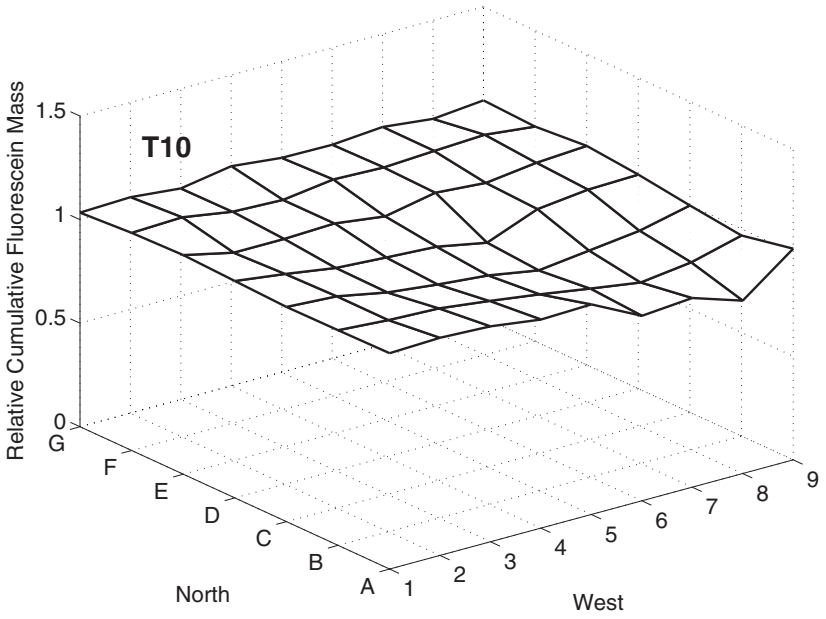

(c)

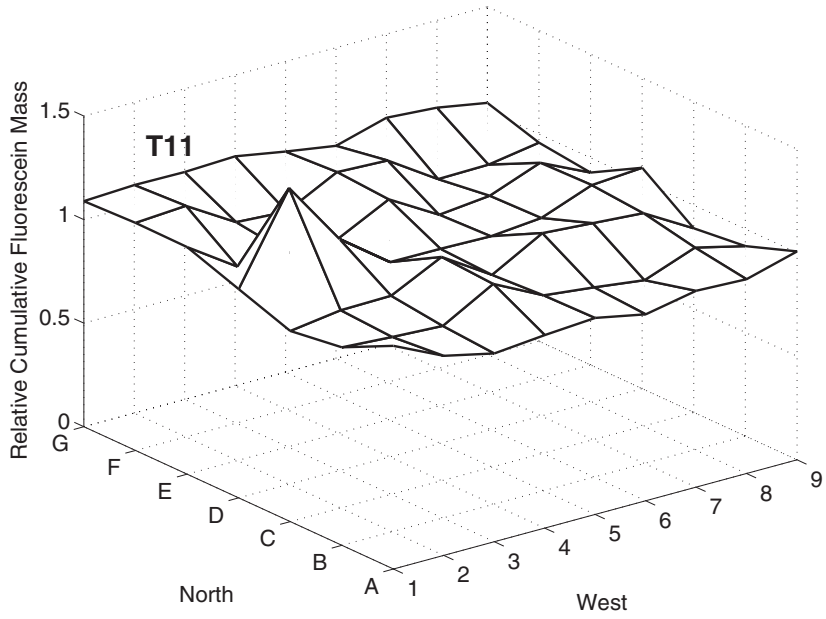

(d)

FIG. 4. (Continued)

and forced conditions were shorter than the exposure time scale, the relationship between the exposure and settling time scales signifies that a portion of the 3 μm particles remained suspended in air when sampling ceased, whereas nearly all of the 14 μm particles would have deposited. It was not possible to evaluate this prediction because the loss of fluorescein in the aerosol release tubing was unknown, and likely varied between the two particle sizes.

These results confirm the general expectation that when the ventilation time scale is sufficiently long, particle deposition will become increasingly uniform as the time scale of the mixing process decreases, and the time scale of the settling process increases.

The difference between T2, and the three other experiments of nominal 3 μm particles released under natural conditions (T1, T3, T4) may be due to variation in convective

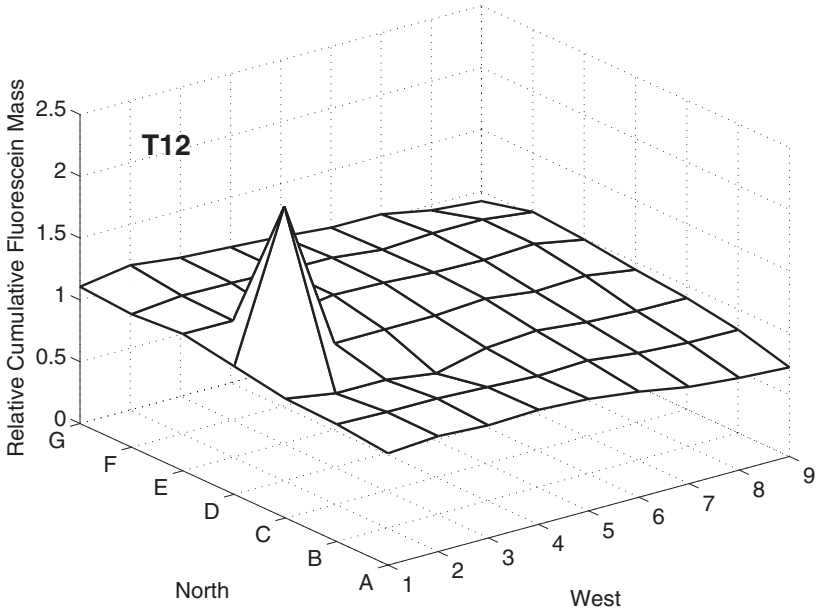

(a)

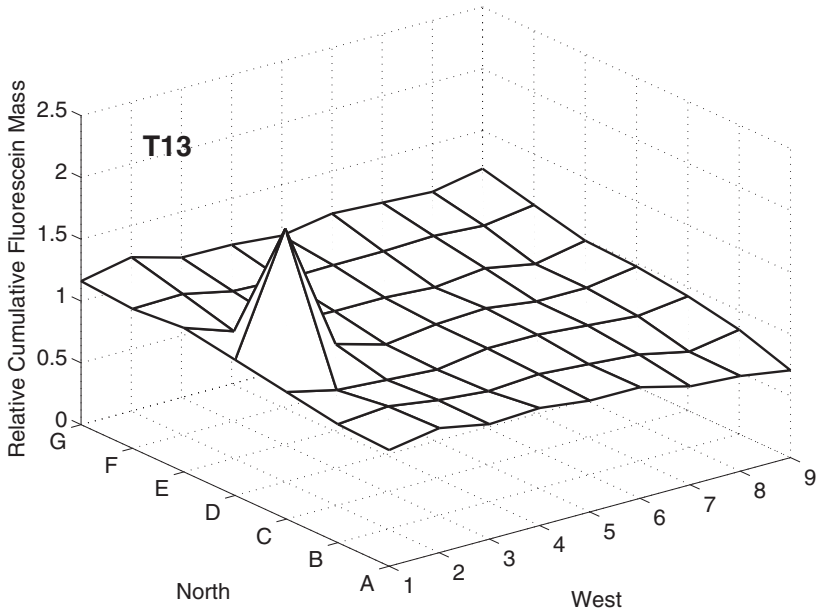

(b)

FIG. 5. Cumulative fluorescein mass deposition, relative to the mean value in each trial, on the chamber floor for particles with nominal $d_a = 14$ μm under forced mixing conditions over 90 min (20 min aerosol release followed by 70 min of deposition). Aerosol was released 0.64 m above the floor at grid point 7C. Mixing was induced by two fans blowing towards each other on the floor in grid point 1D. *(Continued)*

flow in the chamber. The floor deposition patterns suggest that convective flow was present in the chamber, likely induced by thermal gradients generated by solar energy transferred through the building exterior wall and window. To minimize the transfer of solar energy to the chamber, we covered the room windows with two layers of cardboard; and to minimize day-to-day variability, we repeated the experiments at approximately the same time of day. These precautions appear to have been inadequate to obtain stable conditions in the chamber. Lack of thermal regulation and thermal characterization in the chamber are two limitations of this study. Measurement of thermal gradients or airspeeds in the chamber may have identified unique environmental conditions in T2.

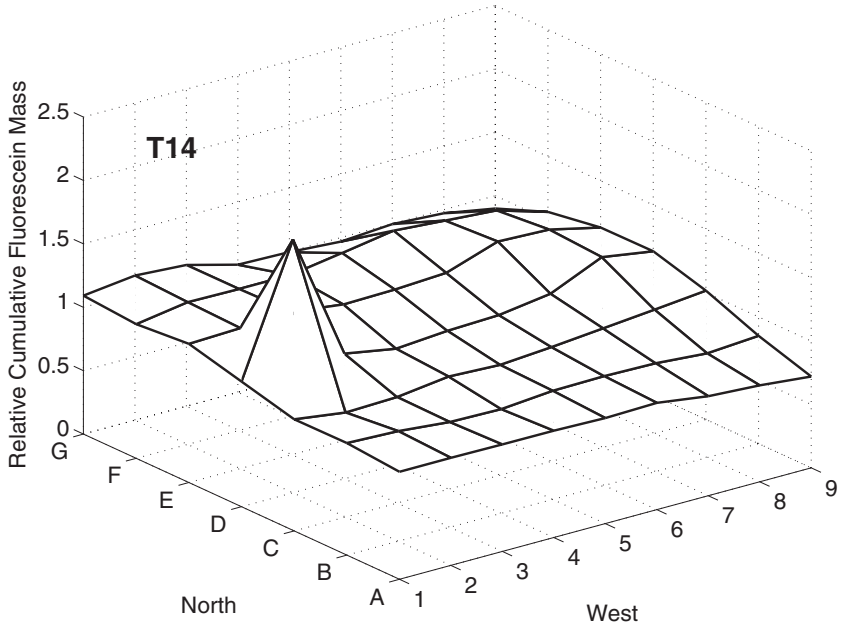

(c)

FIG. 5. (Continued)

The measured size-specific deposition patterns were similar under forced mixing. This will not always be the case: If the time-scale of the mixing process in the forced mixing condition were longer than τ_s of the 14 μm particles, but shorter than τ_s of the 3 μm particles, more spatially heterogeneous deposition patterns would be apparent for the two particle sizes.

Taking advantage of the high sampling frequency and ease of deployment of the ultrasonic anemometers, we measured the advective and turbulent flow in the chamber. Collection of these data is an improvement over previous studies: For example, Sajo et al. (2002) only characterized advection in the environment studied. Advection and turbulence data serve as inputs for zonal models of contaminant transport, and can be used to evaluate CFD simulations. The turbulence in the forced mixing condition was relatively homogeneous, with fluctuating speeds of approximately 3 cm/s. The airspeeds varied, decreasing with distance from the fan, but were generally less than 10 cm/s. These airspeeds are typical of indoor domestic environments, and workplaces (Baldwin and Maynard 1998; Matthews et al. 1989). The turbulence and velocities measured in the chamber core suggest that contaminants could become well mixed throughout the chamber: This was confirmed by the mixing time measured using carbon monoxide tracer studies and by the relatively uniform deposition of the 3 μm and 14 μm particles. High velocity gradients were measured near the mixing fans, and larger particles would be expected to deviate from the streamlines at these locations due to their momentum. This was confirmed by the relatively high fluorescein deposition measured near the mixing fans in trials with the 14 μm particles.

Though there was some difference in the particle sizes measured by the APS and expected from the VOAG operating parameters, the impact on utility of the data for model evaluation is minimal due to the relatively small difference in the estimated terminal settling velocities. Our use of mono-dispersed particles, and collection of airflow data through anemometry and mixing time has generated a unique set of data describing the transport and fate of supermicrometer particles in a room-scale indoor environment. While the use of poly-dispersed particles, such as have been used by Sajo et al. (2002) and Sze To et al. (2008), may increase the realism of the experiment, they significantly increase the challenge of model evaluation.

Though this study was motivated by our interest in the transmission of infectious diseases, and the fate of expiratory particles, our immediate purpose was to develop a data set for the evaluation of contaminant fate and transport models. We hope that the simple geometry of the chamber and release mechanism will allow other investigators to focus on particle-specific challenges of modeling transport, and that future work will better reflect the real-life contexts of disease transmission.

REFERENCES

Atkinson, M., and Wein, L. (2008). Quantifying the Routes of Transmission for Pandemic Influenza, *Bull. Math. Biol*. 70:820–867.

Baldwin, P., and Maynard, A. (1998). A Survey of Wind Speeds in Indoor Workplaces, *Ann. Occup. Hyg*. 42:303–313.

Bémer, D., Callé, C., Godinot, S., Régnier, R., and Dessagne, J. (2000). Measurement of the Emission Rate of an Aerosol Source—Comparison of Aerosol and Gas Transport Coefficients, *Appl. Occup. Environ. Hyg*. 15:904–910.

Berglund, R., and Liu, B. (1973). Generation of Monodisperse Aerosol Standards, *Environ. Sci. Technol.* 7:147–152.

Chao, C., and Wan, M. (2006). A Study of the Dispersion of Respiratory Aerosols in Unidirectional Downward and Ceiling-Return Type Airflows Using a Multiphase Approach, *Indoor Air*. 16:296–312.

Duguid, J. (1946). The Size and Duration of Air-Carriage of Respiratory Droplets and Droplet-Nuclei, *J. Hyg. (Lond)* 4:471–480.

Li, Y., Duan, S., Yu, I., and Wong, T. (2004). Multi-Zone Modeling of Probable SARS Virus Transmission by Airflow Between Flats in Block E, Amoy Gardens, *Indoor Air.* 15:96–111.

Loudon, R., and Roberts, R. (1967). Droplet Expulsion from the Respiratory Tract, *Am. Rev. Respir. Dis*. 95:435–442.

Lu, W., and Howarth, A. (1996). Numerical Analysis of Indoor Aerosol Particle Deposition and Distribution in Two-Zone Ventilation System, *Build. Environ*. 31:41–50.

Matthews, T., Thompson, C., Wilson, D., Hawthorne, A., and Mage, D. (1989). Air Velocities Inside Domestic Environments: An Important Parameter in the Study of Indoor Air Quality and Climate, *Environ. Int.* 15:545–550.

Miller, S., and Nazaroff, W. (2001). Environmental Tobacco Smoke Particles in Multizone Indoor Environments, *Atmos. Environ*. 35:2053–2067.

Murakami, S., Kato, S., Nagano, S., and Tanaka, Y. (1992). Diffusion Characteristics of Airborne Particles with Gravitational Settling in a Convection-Dominant Indoor Flow FIeld, *ASHRAE Trans. Res.* 98:82–97.

Nicas, M. and Jones, R. (in press). The Relative Contributions of Four Exposure Pathways to Influenza Infection risk, *Risk Anal.*

Nicas, M., Nazaroff, W., and Hubbard, A. (2005). Toward Understanding the Risk of Secondary Airborne Infection: Emission of Respirable Pathogens, *J. Occup. Environ. Hyg.* 2:143–154.

Noakes, C., Sleigh, P., Escombe, A., and Beggs, C. (2006). Use of CFD Analysis in Modifying a TB Ward in Lima, Peru, *Indoor Built Environ.* 15:41–47.

Richmond-Bryant, J. (2009). Transport of Exhaled Particulate Matter in Airborne Infection Isolation Rooms, *Build. Environ*. 44:44–55.

Richmond-Bryant, J., Eisner, A., Brixey, L., and Wiener, R. (2006a). Short-Term Dispersion of Indoor Aerosols: Can it be Assumed the Room is Well Mixed?, *Build. Environ*. 41:156–163.

Richmond-Bryant, J., Eisner, A., Brixey, L., and Wiener, R. (2006b). Transport of Airborne Particles within a Room, *Indoor Air.* 16:48–55.

Sajo, E., Zhu, H., and Courtney, J. (2002). Spatial Distribution of Indoor Aerosol Deposition Under Accidental Release Conditions, *Health Phys*. 83:871–883.

Shimada, M., Okuyama, K., Kousaka, Y., and Minamino, D. (1991). Experimental Study of Aerosol Deposition in Stirred Flow Fields Ranging from Laminar to Turbulent Flows, *J. Chem. Eng. Jpn.* 24:203–209.

Smolík, J., Lazaridis, M., Moravec, P., Schwarz, J., Zaripov, S., and Zdímal, V. (2005). Indoor Aerosol Particle Deposition in an Empty Office, *Water Air Soil Pollut*. 165:301–312.

Sze To, G., Wan, M., Chao, C., Wei, F., Yu, S., and Kwan, J. (2008). A Methodology for Estimating Airborne Virus Exposures in Indoor Environments Using the Spatial Distribution of Expiratory Aerosols and Virus Viability Characteristics, *Indoor Air.* 18:425–438.

Thatcher, T., Lai, A., Moreno-Jackson, R., Sextro, R., and Nazaroff, W. (2002). Effects of Room Furnishings and Air Speed on Particle Deposition Rates Indoors, *Atmos. Environ*. 36:1811–1819.

Wan, M., Chao, C., Ng, Y., Sze To, G., and Yu, W. (2007). Dispersion of Expiratory Droplets in a General Hospital Ward with Ceiling Mixing Type Mechanical Ventilation System, *Aerosol Sci. Technol*. 41:244–258.

Zhang, Z., and Chen, Q. (2007). Comparison of Eulerian and Lagrangian Methods for Predicitng Particle Transport in Enclosed Spaces, *Atmos. Environ*. 41:5236–5248.

APPENDIX 1. SUPPLEMENTARY DATA TABLES

TABLE A-1

Mean and fluctuating velocities ($(\overline{u}, \overline{v}, \overline{w})$, $(\sigma_u, \sigma_v, \sigma_w)$) and mean and fluctuating speed ($\overline{U}_s$, σ_s) from combined anemometry measurements for each location and height in the forced mixing condition. Mixing was induced by two 0.08 m diameter instrument fans blowing towards each other on the floor in grid point 1D

Grid point	Height (m)	Mean (cm/s) $(\overline{u}, \overline{v}, \overline{w})$		Fluctuating (cm/s) $(\sigma_u, \sigma_v, \sigma_w)$	σ_s	Grid point	Height (m)	Mean (cm/s) $(\overline{u}, \overline{v}, \overline{w})$		Fluctuating (cm/s) $(\sigma_u, \sigma_v, \sigma_w)$	σ_s
1A	0.18	(1, 4, 2)	9	(3, 5, 4)	5	3D	0.18	(0, −4, −3)	8	(4, 3, 4)	19
1B	0.18	(−5, 0, −4)	9	(3, 3, 4)	16	3E	0.18	(4, −5, −1)	8	(3, 2, 3)	18
1C	0.18	(−24, −4, −8)	28	(5, 5, 6)	16	3F	0.18	(3, −2, −1)	6	(2, 2, 2)	11
1D	0.18	(42, −69, 81)	116	(12, 14, 23)	4	5B	0.18	(5, 5, −1)	10	(4, 4, 4)	6
1E	0.18	(22, −6, −3)	25	(3, 4, 3)	15	5D	0.18	(1, 0, 1)	4	(3, 3, 2)	16
1F	0.18	(8, −2, −1)	10	(3, 3, 3)	8	5F	0.18	(1, −1, 1)	3	(2, 2, 2)	14
1G	0.18	(3, 2, 1)	5	(2, 3, 2)	10	7B	0.18	(3, 6, 0)	8	(3, 3, 3)	8
2B	0.18	(−2, −2, −1)	7	(4, 4, 4)	16	7D	0.18	(−2, 0, 0)	4	(2, 3, 2)	12
2C	0.18	(−12, −13, −5)	22	(8, 6, 6)	15	7F	0.18	(−3, −1, 1)	4	(2, 1, 2)	8
2D	0.18	(24, 32, 29)	55	(13, 21, 16)	10	9B	0.18	(−3, −2, −1)	5	(2, 2, 2)	6
2E	0.28	(9, −9, −3)	14	(3, 3, 3)	17	9D	0.18	(−4, −3, −1)	7	(2, 2, 2)	7
2F	0.18	(6, −3, −1)	9	(3, 3, 2)	12	9F	0.18	(−4, −3, 0)	6	(3, 2, 2)	9
3B	0.18	(0, 1, −3)	8	(5, 4, 4)	10	1C	0.63	(12, −5, 3)	18	(9, 7, 9)	15
3C	0.18	(2, 0, −4)	10	(6, 5, 5)	9	1E	0.63	(7, −3, 2)	10	(3, 3, 3)	15

(Continued on next page)

TABLE A-1
Mean and fluctuating velocities (($\overline{u}$, $\overline{v}$, $\overline{w}$), (σ_u, σ_v, σ_w)) and mean and fluctuating speed ($\overline{U}_s$, σ_s) from combined anemometry measurements for each location and height in the forced mixing condition. Mixing was induced by two 0.08 m diameter instrument fans blowing towards each other on the floor in grid point 1D *(Continued)*

Grid point	Height (m)	Mean (cm/s) ($\overline{u}$, $\overline{v}$, $\overline{w}$)		Fluctuating (cm/s) (σ_u, σ_v, σ_w)	σ_s	Grid point	Height (m)	Mean (cm/s) ($\overline{u}$, $\overline{v}$, $\overline{w}$)		Fluctuating (cm/s) (σ_u, σ_v, σ_w)	σ_s
1F	0.63	(3, −1, 8)	10	(4, 4, 4)	21	3D	1.14	(1, −2, −1)	6	(2, 2, 4)	2
2B	0.63	(10, −1, −1)	13	(7, 4, 5)	7	3F	1.14	(2, −1, −2)	6	(3, 3, 4)	3
2C	0.63	(19, −5, 5)	24	(9, 7, 8)	11	5A	1.14	(1, 0, 5)	7	(3, 3, 4)	3
2E	0.63	(5, −5, 1)	9	(3, 3, 2)	12	5B	1.14	(2, −1, 8)	10	(3, 3, 4)	3
2F	0.63	(4, −3, 2)	7	(2, 3, 2)	7	5D	1.14	(2, −1, 2)	7	(3, 2, 6)	4
3D	0.63	(4, −3, −4)	9	(4, 4, 4)	12	5F	1.14	(2, −1, 3)	8	(3, 3, 6)	3
1A	0.79	(8, 0, 3)	11	(5, 4, 4)	5	5G	1.14	(1, −2, 0)	4	(2, 2, 2)	3
1B	0.79	(13, −2, 7)	17	(6, 5, 5)	6	7B	1.14	(1, 0, 10)	11	(3, 2, 4)	4
1F	0.79	(0, −2, 1)	7	(3, 4, 5)	4	7D	1.14	(1, −1, 4)	6	(2, 2, 5)	4
1G	0.79	(1, −2, 8)	10	(3, 3, 3)	3	7F	1.14	(1, 0, 6)	9	(3, 3, 8)	4
2B	0.79	(7, −2, 8)	13	(6, 4, 5)	6	9A	1.14	(2, 0, 11)	11	(3, 3, 4)	3
2C	0.79	(16, −3, 9)	22	(8, 7, 8)	8	9B	1.14	(0, 0, 7)	8	(3, 2, 5)	4
2E	0.79	(3, −5, 1)	8	(2, 2, 2)	2	9D	1.14	(0, 0, 4)	6	(2, 2, 5)	4
2F	0.79	(0, −3, −4)	6	(2, 3, 3)	3	9F	1.14	(0, 0, −1)	6	(3, 3, 5)	3
3B	0.79	(2, −2, 4)	8	(3, 3, 6)	4	9G	1.14	(0, 0, 11)	11	(2, 2, 3)	3
3D	0.79	(1, −4, −3)	7	(2, 3, 3)	3	1A	1.73	(2, 1, 10)	11	(3, 3, 5)	4
3F	0.79	(2, −2, −1)	6	(3, 3, 4)	2	1B	1.73	(1, −1, 7)	9	(3, 3, 5)	4
5A	0.79	(−1, 1, −1)	5	(2, 3, 3)	3	1C	1.73	(0, −1, 3)	5	(2, 2, 3)	2
5B	0.79	(0, −1, 5)	8	(3, 3, 5)	4	1E	1.73	(1, 1, 10)	11	(3, 3, 4)	3
5D	0.79	(2, −2, 1)	6	(3, 2, 5)	3	1F	1.73	(0, 3, 5)	8	(3, 3, 5)	4
5F	0.79	(2, −2, 1)	6	(3, 2, 5)	3	1G	1.73	(1, 3, 9)	11	(3, 3, 4)	3
5G	0.79	(2, −2, 3)	6	(2, 2, 3)	2	2C	1.73	(0, 0, 2)	4	(2, 2, 3)	2
7B	0.79	(0, 1, 3)	6	(3, 2, 5)	3	2E	1.73	(2, 0, 4)	7	(3, 2, 4)	3
7D	0.79	(−1, −1, 0)	4	(3, 2, 3)	3	3B	1.73	(1, −1, 2)	6	(3, 3, 5)	4
7F	0.79	(0, −1, 3)	5	(2, 2, 4)	3	3D	1.83	(0, −2, 0)	5	(3, 2, 4)	3
9A	0.79	(−1, 0, 1)	4	(2, 2, 4)	2	3F	1.73	(1, 1, 0)	6	(3, 3, 5)	3
9B	0.79	(−1, 0, 5)	7	(2, 2, 6)	4	5A	1.73	(0, 3, −1)	5	(3, 3, 3)	3
9D	0.79	(−2, 0, 4)	6	(2, 2, 4)	3	5B	1.73	(1, −1, 5)	7	(3, 3, 5)	4
9F	0.79	(−1, 0, 5)	7	(2, 2, 5)	4	5D	1.73	(1, 0, 3)	7	(3, 3, 5)	4
9G	0.79	(0, 0, 8)	9	(2, 2, 3)	3	5F	1.73	(2, 0, 4)	7	(3, 3, 5)	4
1A	1.14	(5, 1, 9)	12	(5, 4, 5)	5	5G	1.73	(3, −1, 10)	11	(3, 2, 3)	3
1B	1.14	(4, −2, 7)	11	(4, 3, 6)	5	7B	1.73	(1, 0, 5)	9	(3, 3, 7)	4
1C	1.14	(5, −2, 4)	10	(5, 4, 6)	5	7D	1.73	(1, 0, 7)	8	(3, 2, 6)	5
1E	1.14	(1, −2, −3)	6	(3, 3, 3)	3	7F	1.73	(1, −1, 7)	9	(3, 2, 6)	5
1F	1.14	(0, −1, 1)	6	(3, 3, 4)	3	9A	1.73	(0, 1, 0)	5	(2, 3, 4)	3
1G	1.14	(−2, 0, 2)	6	(3, 3, 4)	3	9B	1.73	(0, 0, 5)	8	(3, 3, 6)	4
2C	1.14	(3, −2, −2)	6	(3, 3, 3)	3	9D	1.73	(0, 0, 5)	7	(2, 2, 5)	4
2E	1.14	(3, −2, −3)	6	(2, 2, 2)	2	9F	1.73	(0, 0, 6)	7	(2, 2, 5)	4
3B	1.14	(2, −2, 3)	7	(3, 3, 5)	3	9G	1.73	(0, 0, 8)	8	(2, 2, 5)	5

TABLE A-2
Comulative fluorescein mass deposited 0.02 m^2 foil samplers on the chamber walls, relative to the mean value of the cumulative fluorescein mass deposited on chamber floor over 90 min (20 min aerosol release followed by 70 min of deposition under natural mixing). Samplers were centered 1.12 m above the floor, and centered in each wall, lengthwise

	Relative cumulative fluorescein mass			
Exp	North	East	South	West
T1	0.00	0.00	0.00	0.00
T2	0.00	0.00	0.00	0.22
T3	0.00	0.01	0.00	0.00
T4	0.00	0.02	0.00	0.00
T6	0.00	0.00	0.00	0.00
T7	0.02	0.00	0.00	0.02

TABLE A-3
Time-weighted-average fluorescein mass concentration (C_{TWA}) relative to the mean value in each trial, measured at 1.5 m above the floor over 90 min (20 min aerosol release followed by 70 min of deposition) under natural and forced mixing conditions. Aerosol was released 0.64 m above the floor at grid point 7C. Forced mixing was induced by two 0.08 m diameter instrument fans on the floor, blowing towards each other in grid point 1D

	Relative fluorescein mass C_{TWA}													
	Natural mixing							Forced mixing						
	$d_a \sim 3\ \mu m$				$d_a \sim 14\ \mu m$			$d_a \sim 3\ \mu m$				$d_a \sim 14\ \mu m$		
Grid point	T1	T2	T3	T4	T5	T6	T7	T8	T9	T10	T11	T12	T13	T14
2B	0.96	0.87	1.3	1.4	2.2	1.4	0.84	1.4	0.98	1.1	1.7	0.85	0.64	0.77
2D	1.1	1.4	1.2	0.29	1.8	1.3	1.3	0.44	0.65	1.1	0.70	0.61	0.64	0.98
2F	0.72	1.4	0.90	0.53	1.3	0.87	1.0	1.2	1.5	1.2	1.7	0.68	0.97	0.75
4B	0.46	1.0	1.0	1.4	2.6	2.5	1.7	1.2	1.4	0.66	1.3	0.95	0.76	0.46
4D	0.85	1.1	0.89	0.87	1.5	0.80	1.2	0.65	0.87	0.93	0.43	0.58	0.76	0.99
4F	1.0	1.1	0.85	1.4	0.83	0.47	0.56	1.0	0.94	1.2	0.80	0.75	0.84	0.51
6B	0.98	0.77	1.4	0.56	1.1	1.9	1.7	1.1	0.75	0.66	1.26	1.8	0.96	0.68
6D	0.86	0.60	1.2	0.60	0.37	0.76	0.91	1.0	0.61	1.2	0.86	2.1	1.4	2.3
6F	1.3	0.96	0.36	0.98	0.09	0.46	0.72	1.5	1.0	0.78	0.48	0.76	0.94	0.68
8B	0.98	1.3	1.3	1.7	0.16	0.65	0.19	0.83	0.41	1.03	0.95	1.3	1.1	1.5
8D	1.2	0.91	0.88	1.5	0.12	0.64	0.68	1.2	1.2	0.93	0.95	1.0	1.8	1.6
8F	1.6	0.51	0.72	0.89	0.09	0.33	1.2	0.55	1.6	1.1	0.93	0.56	1.2	0.72
CV (%)	28	29	30	45	87	65	45	33	38	20	41	51	34	55